TITLE: Overview of IRS Plasma Wind Tunnel Facilities

Overview of IRS Plasma Wind Tunnel Facilities

Monika Auweter-Kurtz,
Thomas Wegmann
Universität Stuttgart
Institut für Raumfahrtsysteme
Pfaffenwaldring 31
70550 Stuttgart
Germany

Introduction

Upon entering the atmosphere of celestial bodies, spacecrafts encounter gases at velocities of more than ten km/s, thereby being subjected to great heat loads. Figure 1.1 shows artist's concept of X-38 reentering Earth's atmosphere [1]. The X-38 is a technology demonstrator for the proposed Crew Return Vehicle (CRV), which will be designed for an emergency return from the International Space Station.

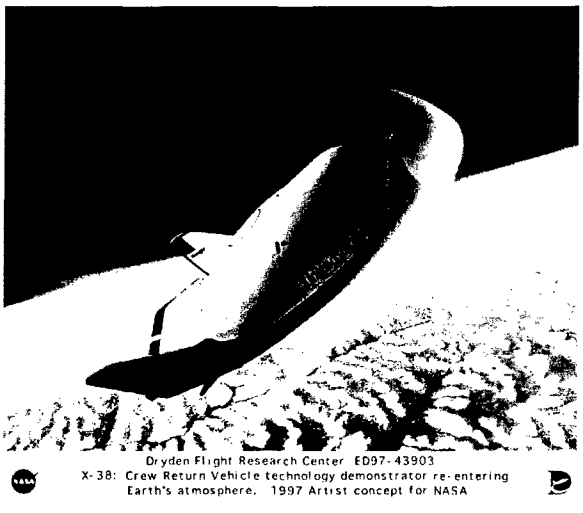

Fig. 1.1: X-38 re-entering Earth's atmosphere [1]

The task of a thermal protection system (TPS) is to protect the substructure of the vehicle against local and global overheating.

A heatshield material should have:

- a low mass,
- a smooth surface to avoid an early flow change from laminar to turbulent,
- the necessary strength to withstand aerodynamic, aeroelastic, chemical and heat loads,
- material catalycity be as low as possible, that is it should not encourage the recombination of oxygen and nitrogen or nitrogen oxide formation,
- an emissivity as high as possible, at least 0.8, in order to reject a large portion of the heat input at the lowest possible temperature.

For the qualification of heatshield materials regarding these requirements a lot of different ground testing facilities are necessary which cannot all be discussed during this lecture. This lecture concentrates on the plasma wind tunnel facilities (PWK) which have been in use at the IRS (Institut für Raumfahrtsysteme of Stuttgart University) for more than a decade [2, 3]. Firstly, they are used for the qualification of heatshield materials in regard to chemical and high enthalpy loads occurring during reentry into the earth's atmosphere and entry into other planetary atmospheres [4 - 8]. Secondly, they are tools for the development of reentry measurement techniques [9 - 12]. In addition, these facilities can be used for the validation of numerical codes [13 - 16].

In ground test facilities the simulation of the real gas composition as it is set up near the surface of the spacecrafts and probes is only possible for a few ms with free ballistic ranges. Resulting measurement times are of only a few µs. So-called hot shot tunnels [17] or piston shock tunnels [18] offer measurement times of a few ms, but due to the high gas temperature of the oncoming flow predissociation cannot be avoided. The duration of test runs within these facilities is far too short for the development and testing of heat protection materials since the surface largely remains cold and therefore hardly interacts with the hot gas.

For the development of heat protection materials for entry bodies one, therefore, depends on plasma wind tunnels, which do not offer a complete simulation of entry conditions. Because of a restriction of the arc chamber pressure and the strong nonequilibrium phenomena in the arc tunnels it is in principle impossible to correctly simulate the flight environment, which means characteristic Reynolds number and Mach number, for the first phase of reentry (Fig. 1.2).

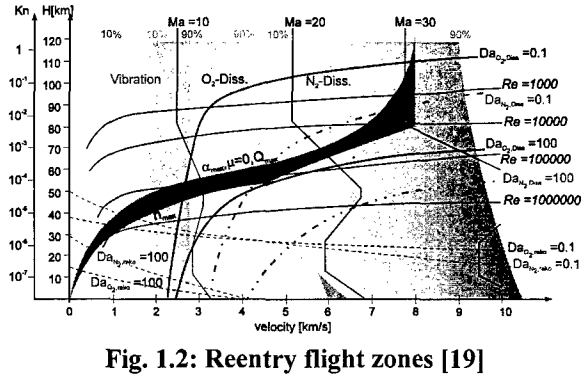

Fig. 1.2: Reentry flight zones [19]

Paper presented at the RTO AVT Course on "Measurement Techniques for High Enthalpy and Plasma Flows", held in Rhode-Saint-Genèse, Belgium, 25-29 October 1999, and published in RTO EN-8.

With the exception of tunnels operating at high ambient pressure and able to simulate the flight conditions of the last phase of reentry, a plasma wind tunnel has to be seen as a tool for the simulation of the flow near the material surface. Therefore, the goal has to be the duplication of the conditions near the surface of a vehicle which have to be determined first by calculation or by a flight experiment (Fig. 1.3). Such wind tunnels are then suitable for the development of TPS materials.

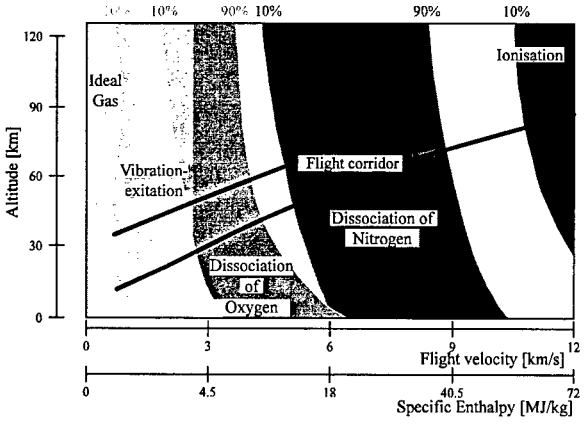

Fig. 1.3: Reentry flight conditions

With plasma wind tunnels a continuous stream of plasma of high specific enthalpy and velocity is produced with the help of thermal or magnetoplasmadynamic generators (TPG or MPG). Our plasma wind tunnels PWK 4 and PWK 5, equipped with thermal arc generators (TAG), are suitable for the studies of aerodynamic loads of high enthalpy flows. High impact pressures and fairly high Mach numbers and specific enthalpies can be generated. However, the exhaust velocity is limited to several km/s and low impact pressures cannot be achieved. The erosion rate of heat protection material with an oxidation protection coating (defined as mass loss per exposed area and time) is especially high at low pressure levels and, therefore, in regions of high velocities [20 - 22]. These conditions can be simulated with the help of MPGs in PWK 1 and PWK 2.

The inductively heated PWK 3 is used for basic research on TPS materials, especially regarding their catalytic behavior, because no plasma impurities occur from electrode erosion. In addition, tests in a pure oxygen or in a mainly CO_2 atmosphere, for example for entry into Mars' or Venus' atmosphere, can be performed [23, 24].

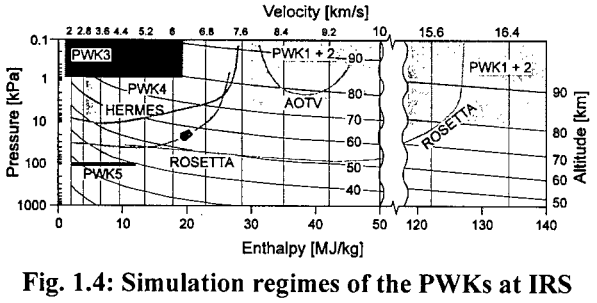

Fig. 1.4: Simulation regimes of the PWKs at IRS

The simulation regimes of the PWKs at IRS can be seen in Figure 1.4 together with some typical reentry trajectories.

A PWK must be able to be used for the following:

- qualification of TPS materials,
- basic research on TPS materials,
- verification of numerical codes,
- development and qualification of diagnostics methods,
- development and qualification of flight experiments.

It is of the utmost importance that the impurity level in the plasma is as low as possible and especially materials of high catalycity, as for example copper, have to be avoided as this would lead to a falsification of the results.

2. Simulation Requirements for Reentry Vehicles

For the development of thermal protection systems for reentry bodies especially the oxidation behavior of TPS materials has to be studied, in particular if the vehicle has to be designed as a reusable one. For this purpose facilities are needed to simulate in steady state conditions the required surface temperature on the material, pressure, specific enthalpy and mass flow rate.

First the simulation requirements for a small winged reentry vehicle will be shown and discussed. For re-usable winged space vehicles like HERMES, HOPE or CRV the heat loads and therefore also the chemical loads are highest at the nose cap and at the leading edges. For HERMES, which was studied in Europe during the 80s, most data are available and is therefore used here as an example. Based on the tra-

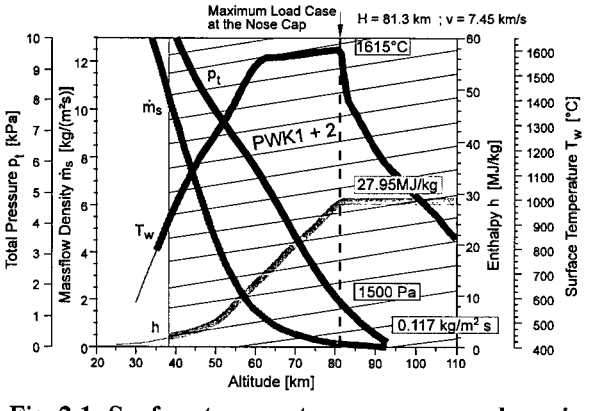

Fig. 2.1: Surface temperature, pressure and specific enthalpy at the nose cap of HERMES during reentry for landing in Istres and the required mass flow within the PWK. (Thick lines: simulation region with PWK 1 or PWK 2, hatched zone: simultaneous simulation with PWK 1 or PWK 2)

jectory of HERMES the pressure, density and the specific enthalpy of these surface elements was calculated [5]. The surface temperature, pressure and specific enthalpy are shown as a function of altitude in Fig. 2.1 for the nose cap and in Fig. 2.2 for the leading edge.

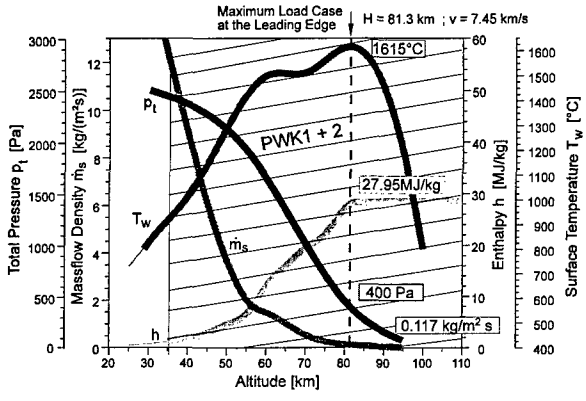

Fig. 2.2: Surface temperature, pressure and specific enthalpy at the leading edge of HERMES during reentry for landing in Cayenne and the required mass flow within the PWK. (Thick lines: simulation region with PWK 1 or PWK 2, hatched zone: simultaneous simulation with PWK 1 or PWK 2)

Candidate TPS materials of modern reusable vehicles are of carbon fiber with carbon or SiC matrixes and an oxidation protection coating on top which in most cases again consists of SiC. The erosion of these materials is most severe at high temperature and low pressure levels due to active oxidation [20 - 22]. These conditions can be duplicated with the help of an MPG as used in the plasma wind tunnels PWK 1 and PWK 2. The surface temperature, pressure and specific enthalpy regions of the trajectory which are achievable with these facilities are marked in Figs. 2.1 and 2.2 by a thick line. The density and velocity profile together with the cross section of the plasma beam of PWK 1 and PWK 2 of ca. 0.031 m^2 lead to the required mass flow for these tunnels, which is included in Figs. 2.1 and 2.2. The hatched zone marks the region where surface temperature, specific enthalpy, pressure and mass flow rate can be duplicated simultaneously. In the case of the leading edge, this region is limited by the maximum possible mass flow whereas in the case of the nosecap the maximum achievable stagnation pressure is the limiting factor. But for both cases the low pressure and high temperature phase of the reentry can be simulated including the maximum temperature point.

If the gas were in thermodynamic and chemical equilibrium near the material surface during reentry and within the test facility, this simulation with the help of a magnetoplasmadynamic wind tunnel would be perfect. In both situations this is not the case and for both situations the exact gas composition is still unknown today. But a lot of research programs are under way so that in the future more knowledge will be gained in this area. With the help of computer programs in which non-equilibrium chemistry is included, the reentry situation as well as the MPG wind tunnel situation is being simulated [14, 25]. At the same time, measurement techniques are being developed for the analysis of the high enthalpy gas during the material tests in ground based facilities [26, 27] as well as during the vehicle reentry [9-12].

Compared to the trajectory of a winged spacecraft like HERMES, the reentry of a ballistic or semiballistic space capsule from a low earth orbit is marked by essentially higher heat loads due to the steeper ascent. Figure 2.3 shows the heat flow on the wall, the pressure at the stagnation point, the mass flow and the specific enthalpy all dependent on the altitude. Because the reuse of a space capsule has not been demanded yet, ablation materials are normally used for the thermal protection shield. On the German-Japanese EXPRESS mission, launched in 1995, a first experiment was conducted to determine whether ceramic thermal protection materials can be used in order to enlarge the possibility of reentry measurement techniques. A C/C-SiC tile for the stagnation point region, manufactured by the DLR Stuttgart, was qualified during the flight [28].

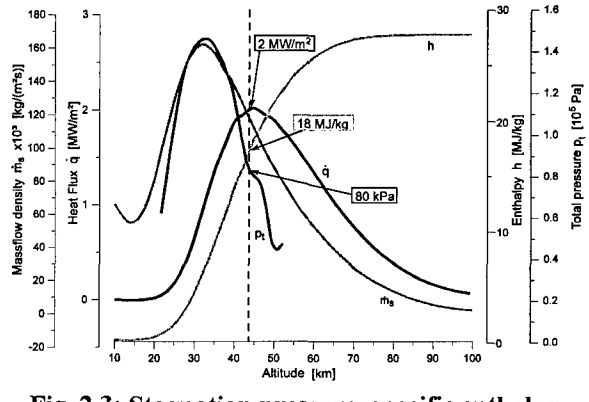

Fig. 2.3: Stagnation pressure, specific enthalpy, heat flux and mass flow density for the nose cone of EXPRESS as a funtion of the altitude

The EXPRESS capsule is a typical example of a ballistic, reentry capsule protected by an ablator. The hot reentry phase, which can be simulated in a ground facility like a plasma wind tunnel, begins at a nominal height of 100 km at a speed of approximately 7.4 km/s. The heating during the capsule's descent was calculated according to the results from earlier flights performed by the manufacturers from the Russian company Khrunichev. The maximum was expected at a heat load of 2 MW/m^2 after 235 s at a height of 45 km. At this point in time the stagnation point pressure should be about 75 kPa. The maximum stagnation pressure of 15 MPa should be reached after approximately 275 s. The capsule would at this point be at a nominal height of 32 km. The maximum stagnation pressure cannot be reached in the IRS PWKs equipped with MPGs. However, the heat flow

profile is fully feasible. Figure 2.4 shows the course of the heat flow during reentry as well as the course of the heat flow as simulated in the PWK. Because ceramic thermal protection was used at the tip of EXPRESS, maximum erosion at low pressure and high temperature was to be expected just as with HERMES. Therefore, using the MPG tunnel the worst case was examined.

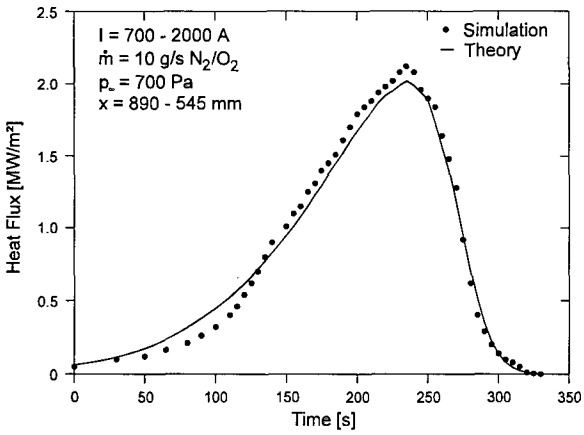

Fig. 2.4: Heat flux profile of the EXPRESS mission

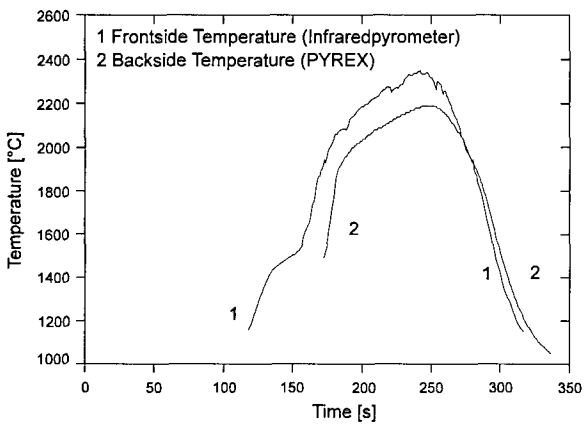

Fig. 2.5: Surface temperature of the ceramic heat shield of the EXPRESS capsule in the PWK

During the flight qualification of the EXPRESS experiments, maximum surface temperatures of approximately 2300°C (see Fig. 2.5) resulted from a duplication of the heat flow profile in the MPG-tunnel at the IRS. The front and rear temperatures of the ceramic tile were measured pyrometrically. The rear temperature was to be determined by an EXPRESS experiment - the miniature pyrometer PYREX from the IRS [9].

At the IRS a semi-ballistic capsule COLIBRI (Concept of a Lifting Body for Reentry Investigations) was designed as a testbed to perform autonomously scientific and technology experiments during the reentry flight [29] with three primary goals:

- to investigate aerothermodynamic phenomena encountered during hypersonic flight,
- to test advanced materials and concepts for thermal protection systems, and
- to perform both flight dynamics and navigation as well as guidance, and control experiments during a controlled atmospheric flight.

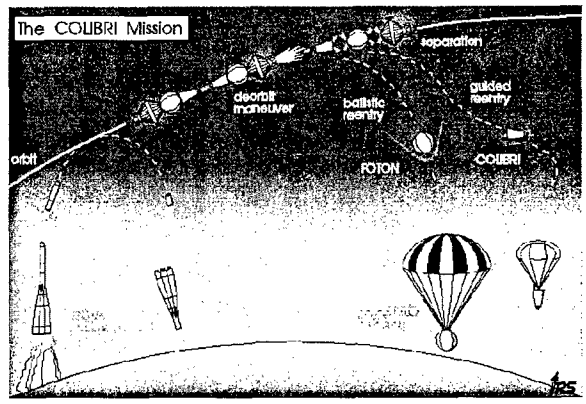

Fig. 2.6: The Colibri Mission [29]

The mission profile of the COLIBRI capsule is illustrated in Fig. 2.6. A "piggy-back"-flight opportunity on a Russian FOTON carrier-capsule was considered for this study that would be launched into a low Earth orbit by a Soyuz rocket. The drawback associated with this low-coast approach is that entry conditions are defined by the ballistic FOTON capsule to be recovered in southern Russia and can not be selected independently. Thus, the recovery area of FOTON is at the lower end of the attainable landing area of the semi-ballistic COLIBRI vehicle as illustrated in Fig. 2.7. Though FOTON enters the atmosphere following a ballistic path, the reentry flight of COLIBRI will be autonomous and controlled. In order to ease the recovery of the vehicle, a landing accuracy of 5 km is regarded as sufficient.

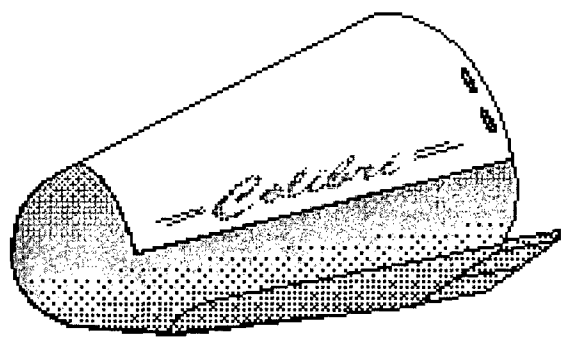

Fig. 2.7: The COLIBRI capsule [29]

An example of the calculated conditions for the semiballistic Colibri capsule project is shown in Fig. 2.8. The maximum heat flux of ~ 2.2 MW/m^2 is expected at a stagnation pressure of 20 kPa and a corresponding specific enthalpy of 26 MJ/kg. These conditions are well within the simulation region of the plasma wind tunnel PWK 4, equipped with the thermal plasma generator RB3.

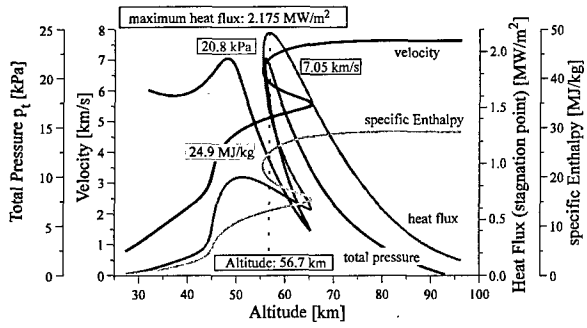

Fig. 2.8: Total pressure, velocity, heat flux and specific enthalpy vs. altitude for the COLIBRI reentry mission [29]

Huygens is an European probe which will be used to investigate the atmosphere of the Saturnian moon Titan. It is being carried to the Saturn system with the Cassini spacecraft, which was designed, built and launched by NASA [30]. During the entry into Titan's atmosphere, the probe has to be decelerated aerodynamically from about 6.1 km/s to 400 m/s within three minutes. This will be done by a heat shield with a diameter of 2.7 m. In Fig. 2.9 the heat flux, specific enthalpy and dynamic pressure of a typical probe trajectory are plotted versus the altitude.

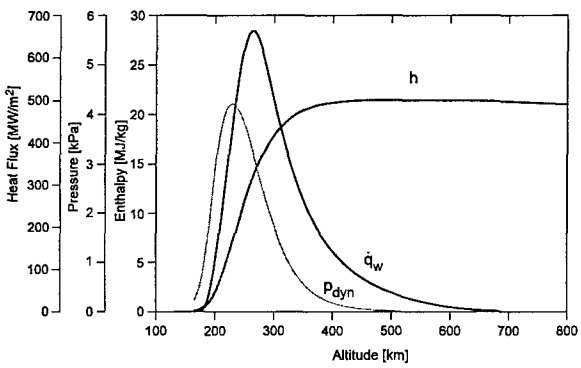

Fig. 2.9: Heat flux, pressure and specific enthalpy profiles for the entry of Huygens into the atmosphere of Titan [7]

These conditions can be completely simulated in a PWK equipped with an MPG at the IRS [7, 8]. For this mission the composition of Titan's atmosphere presented a special challenge for the test facilities. The atmosphere consists of approximately 80 - 90 % nitrogen, 3 - 10 % methane and presumably about 10 % argon. Carbon based gases are very difficult to handle in plasma generators because the carbon settles on the electrodes especially when they are water-cooled. The erosion caused by carbon is large if it is in contact with hot glowing cathodes. Therefore, special measures were necessary to avoid any contact of the glowing tungsten cathode with carbon, to assure the anode attachment and to avoid short cuttings of isolated generator segments due to a carbon layer formation. In the IRS MPG facility continuous operation with methane components up to 10%, as required, could be reached for several hours.

The capability of the IRS plasma wind tunnels to produce plasma flows of an enthalpy level of more than one hundred MJ/kg can be used to duplicate the stagnation point flow field of very fast space vehicles as expected for the reentry flight of a comet sample return probe like ROSETTA (see Fig. 2.10) or of a Mars or Venus sample return probe [31]. In case of a comet sample return mission the earth entry velocity of the probe is in the range of about 15 km/s. This yields a specific enthalpy of about 130 MJ/kg and a maximum heat flux to the probe of more than 20 MW/m^2. During the aerobraking maneuver of a sprint-type manned Mars mission similar values of the quantities mentioned above are expected (see Fig. 2.11)

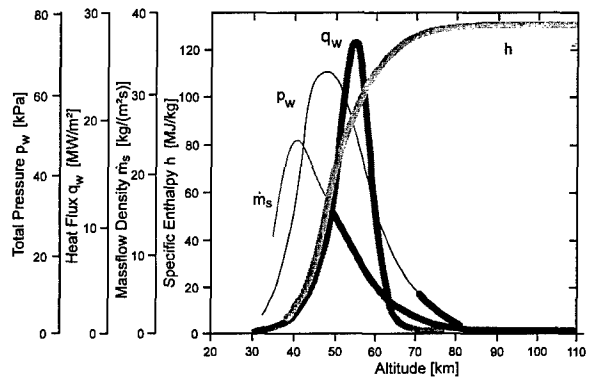

Fig. 2.10: Heat flux, pressure, specific enthalpy profiles and mass flow rate for the reentry of ROSETTA [31]
(Thick lines: simulation region with PWK)

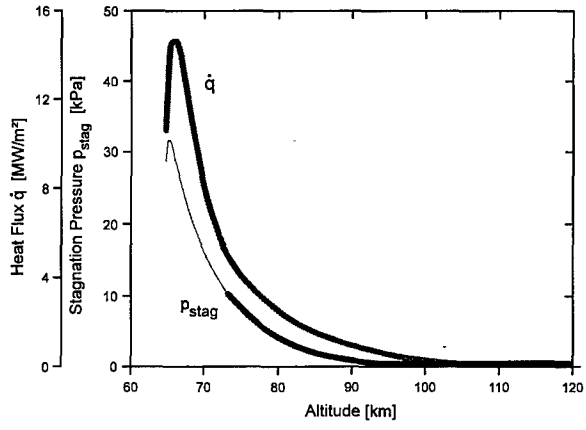

Fig. 2.11: Heat flux and stagnation pressure profiles during aerobraking flight of a sprint type Mars mission in the Earth's atmosphere [31]
(Thick lines: simulation region with PWK)

3. Plasma Wind Tunnels

The term plasma wind tunnel is to be understood as a stationary test facility in which a high enthalpy flow is produced with the help of a plasma generator. The operating times range typically from several minutes to several hours. Arc-driven high enthalpy shock tube tunnels, such as the ONERA High En-

thalpy Wind Tunnel F4 [32], which like other shock tube tunnels have operating times of a few milliseconds, are actually plasma wind tunnels too. But today they are put in a class with the shock tube tunnels. There are various types of plasma wind tunnels, depending on the kind of plasma generator used.

As already pointed out it is basically impossible to create a complete simulation of all gas parameters with plasma generators. The combustion chamber pressures necessary for this would be around 10 GPa. It is not primarily the mechanical loads which makes this impossible. With continually operated arcjet accelerators the pressure is principally limited to 1 MPa up to approximately 10 MPa. At such a pressure level already a nitrogen arc with a diameter of 1 cm and a temperature of 20 kK is optically thick [33]. This means that the arc changes into a radiation source which according to the Stefan-Boltzmann Law radiates proportionately T^4 almost like a black body radiator. When, however, the radiation losses are so extremely high, the device can, on the one hand, not be cooled and on the other hand every increase of the arc energy leads to a drastic increase of the radiation losses and, in contrast to this, only to a small increase of plasma flow enthalpy which is emitted from the device. Thus for material development for the thermal protection of entry bodies one is dependent on plasma wind tunnels that do not offer a complete simulation of entry conditions. Therefore, one equips varied tunnels so that the influence of individual aspects which are important for material investigations can be estimated. These tunnels can be operated for minutes or for hours on end, whereby the specific enthalpy, the pressure, the heat flux, the wall temperature and the concentrations of the most important plasma components can be reproduced near the surface.

A plasma wind tunnel consists of the following components:

- a vacuum tank at IRS equipped with a moveable platform for positioning of the TPS sample,
- a vacuum pump system for creating the low ambient pressure necessary for the simulation,
- a plasma generator to create the high enthalpy plasma flow,
- a suitable power supply system, usually a rectifier plant, or a high frequency generator,
- the auxiliary components such as a gas and cooling water supply at different pressures, emission purifier etc.,
- and the measurement equipment and data processing system.

As an example for the facilities at IRS the scheme of the PWK 1 facility can be seen in Fig. 3.1. Figure 3.2 shows a photograph of PWK 1.

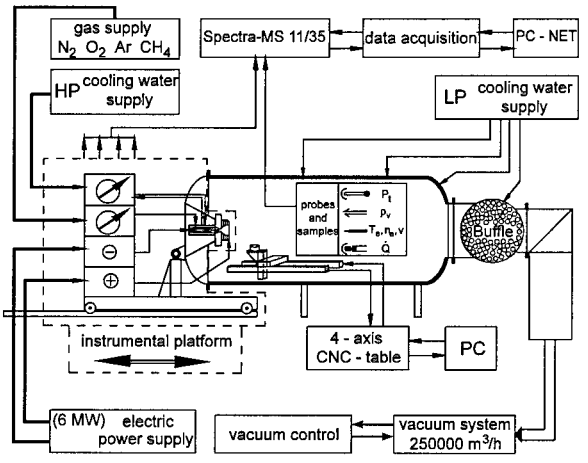

Fig. 3.1: Scheme of plasma wind tunnel PWK 1

The vacuum tank used for the plasma wind tunnel PWK 1 is a 5 m long steel tank with a diameter of 2 m, divided into three cylindrical segments all of which have a double-wall cooling. The connection between the last two segments is protected against heat by a water-cooled copper shield.

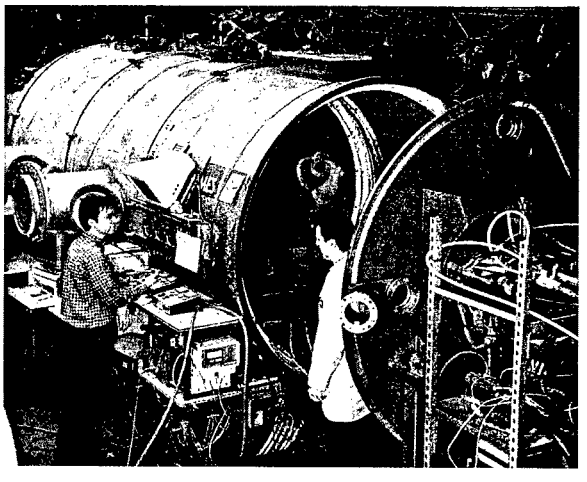

Fig. 3.2: The plasma wind tunnel PWK 1

The tank is closed with a hemispherical part which is connected to the vacuum system (see section 3.2) and protected against heat by water-cooled copper shields. On the other side the vacuum chamber can be opened by moving the plane cover plate on a guide rail. The plasma source is not located in the vacuum tank, but flanged on a conical part of the plate. The cone-shaped element of the end plate enables the plasma source to be fixed at that point. The whole plasma jet range is accessible by optical methods.

The tank is equipped with a 4-axis positioning system on which the different probes and the specimen support system can be mounted. This allows the simulation of parts of the reentry trajectories by moving the specimen in the plasma flow.

Windows with optical glass allow pyrometric temperature measurements on the front side of the specimen at distances from the plasma source between about 50 mm and 1000 mm. Moreover, spec-

troscopic measurements perpendicular to the plasma jet axis are possible through three movable flanges of three optical glasses each, which are located on both sides of the tank opposite each other and on the top (see Fig. 3.2).

An additional vacuum tank of identical size and with the same equipment is available in a second laboratory of IRS (Fig. 3.3). However, this vacuum tank consists only of one segment, made of stainless steel, to prevent corrosion caused by atomic oxygen.

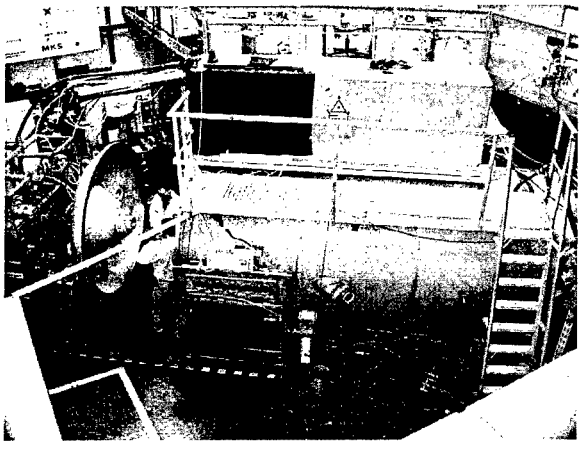

Fig. 3.3: The plasma wind tunnel PWK 2

As long as the above described vacuum tanks are equipped with magnetoplasmadynamic generators (section 4.2), these plasma wind tunnels are called PWK 1 or PWK 2, respectively. If, instead, a thermal plasma generator (section 4.1) is used, they are called PWK 4.

The whole experimental setup of PWK 3, shown in Fig. 3.4, consists of the inductively heated plasma source IPG3 (section 4.3) and the vacuum chamber. The size of this vacuum chamber is about 2 m in length and 1.6 m in diameter. Material support systems and mechanical probes can be installed onto a moveable platform inside the tank. Optical accesses to the vacuum chamber are provided in order to observe the plasma flow and to perform optical diagnostics. As can be seen in Fig. 3.5, the plain lid of PWK 3 is to carry the plasma generator and the external resonant circuit, which contains the capacitors with the connection to the plasma generator.

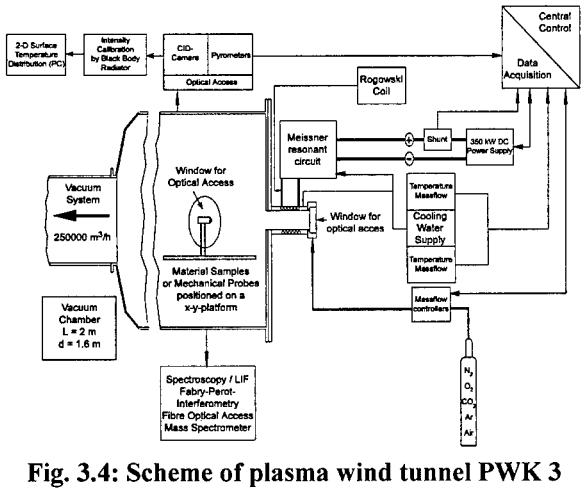

Fig. 3.4: Scheme of plasma wind tunnel PWK 3

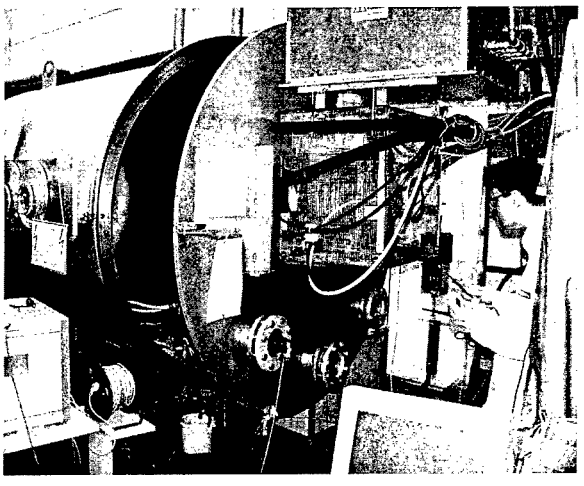

Fig. 3.5: The plasma wind tunnel PWK 3

All the plasma wind tunnels PWK 1 - 4 are connected to the central vacuum (section 3.2), the central power (section 3.1) and the central gas supply system.

The plasma wind tunnel PWK 5, also equipped with a thermal plasma generator (section 4.1), is not connected to a vacuum system. Thus, this test facility is suitable for testing TPS materials at pressure levels higher than 10^5 Pa. The scheme of PWK 5 can be seen in Fig. 3.6.

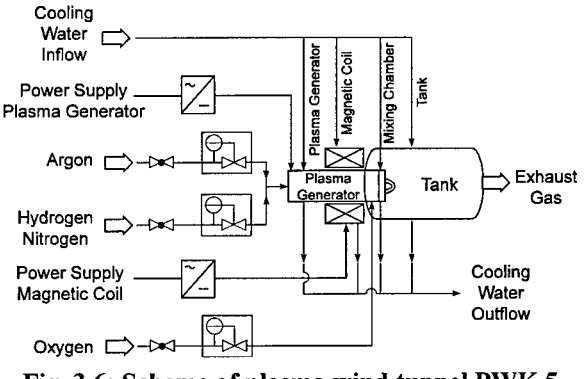

Fig. 3.6: Scheme of plasma wind tunnel PWK 5

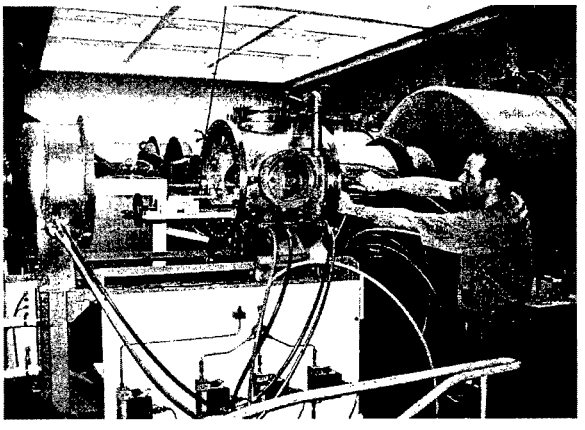

Fig. 3.7: The plasma wind tunnel PWK 5

The tank of PWK 5 (Fig. 3.7) is a 0.7 m long steel chamber with a diameter of 0.5 m, equipped with

double-wall cooling. It is equipped with a specimen support system which is moveable manually along the plasma flow. Also the PWK 5 is connected to the central power supply and gas supply system.

3.1 Power supplies

The electric power for the arc plasma generators is supplied by a current-regulated thyristor rectifier consisting of six identical units supplying 1 MW each (Figs. 3.8 - 3.9). These may be connected in series or parallel, thus varying the desired output level of current, voltage, and power. The current ripple is less than 0.5 %. The maximum current is 48 kA supplied at 125 V and the maximum voltage is 6000 V at a current of 1000 A.

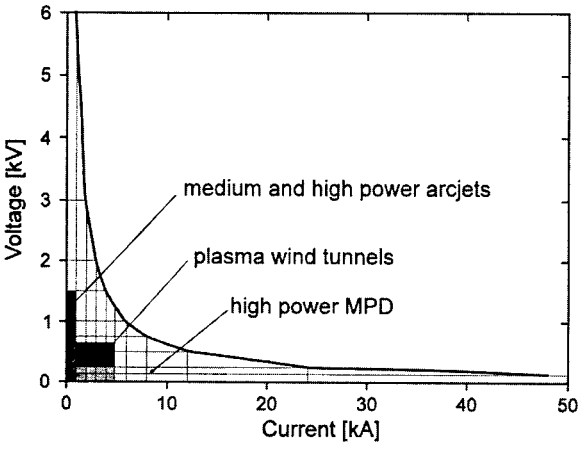

Fig. 3.8: Voltage vs. power characteristic of the power supply system

Fig. 3.9: High voltage thyristor units of the power supply system

For the inductively heated plasma wind tunnel PWK 3 a radio frequency generator with a primary power of 400 kW is used. This device allows the operation of an induction coupled plasma generator with a coil power of 150 kW at a nominal frequency of 650 kHz. An external resonance circuit is designed for an optimal coupling into the plasma over a wide pressure range with different gases.

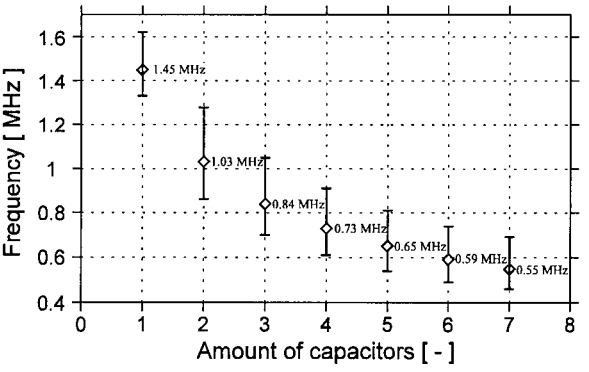

Fig. 3.10: Nominal operating frequencies for different capacitor switchings

The resonant circuit is built in Meissner type switching [34] using a metal-ceramic triode with an oscillator efficiency of about 75 % [35]. Its nominal frequency can be changed by switching the order or the number of capacitors (see Fig. 3.10) as well as by the use of coils with different inductivities. A maximum of 7 capacitors with a capacity of 6000 pF ± 20% each can be connected. The external resonant circuit is cooled by a high pressure water cooling circuit. The error bars in Fig. 3.10 take into account the tolerances of the capacitors. For the present investigations it is tuned to a nominal frequency of 0,55 MHz using a water-cooled 5-turn coil with a length of about 120 mm. The incoming anode power can be adjusted by the control of the anode voltage.

3.2 Vacuum System

A vacuum pump system is used to simulate pressures at altitudes up to 90 km. This pumping system consists of four stages: the first two stages consist of roots blowers, the third stage is a multiple slide valve type pump, and the last stage (pumping up to atmospheric pressure) is a rotary vane type pump (Figs. 3.11 - 3.12). The total suction power of the pumps amounts to 6000 m^3/h at atmospheric pressure and reaches about 250000 m^3/h at 10 Pa measured at the intake pipe of the system, which has a diameter of

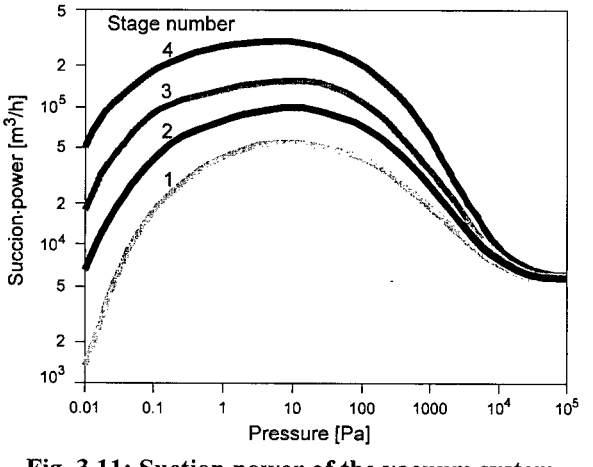

Fig. 3.11: Suction power of the vacuum system

1 m. The base pressure of the system is 0.5 Pa. The

desired tank pressure can be adjusted between the best achievable vacuum and 100 kPa by removing one or more pumps from the circuit and/or mixing additional air into the system close to the pumps.

Fig. 3.12: Roots pump stage (4th stage) of the vacuum system

4. Plasma Generators

Two plasma generator concepts, the thermal and the magnetoplasmadynamic generator (TPG and MPG), are in use in the arc heated plasma wind tunnels; they mainly differ in the acceleration concept.

In thermal arc generators (TAG) the test gas is heated by means of an electric arc and usually accelerated through a Laval nozzle. Regarding magnetoplasmadynamic generators (MPG), additional electromagnetic forces are used to accelerate the test gas. The inductive plasma generator (IPG) also belongs to the group of TPGs. With this electrodeless design the plasma is produced by inductive heating using a radio frequency generator. With the TPG, where the gas is first constricted into a kind of chamber, the hypothetic chamber conditions p_0, h_0 and T_0 may be used as reference parameters. This does not make sense with an MPG, where magnetic acceleration occurs in the nozzle.

4.1 Thermal arc generators (TAG)

Thermal arc generators for wind tunnel applications are run at high pressures, high mass flows and an electric power of up to 100 MW [36]. In order to keep the electrode losses and especially the erosion of the cathode to a minimum, the current intensity of the TAG should be kept as low as possible. As a result the voltage is high. The electrodes of those apparatus that are used for the simulation of reentry into the earth's atmosphere are mostly water-cooled and usually made of copper. During the simulation of atmospheres without oxygen components, hot, glowing cathodes made of thoriated tungsten may be employed, their advantage being an extremely low rate of erosion.

The erosion of the cold cathodes is relatively high and influences the quality of the plasma flow. Especially copper particles are unwanted in the plasma since they may be deposited on the material that still has to be examined and they possibly influence the catalycity of the samples. In addition, in the case of water-cooled cathodes, a locally settled arc attachment spot on the cathode leads to its destruction. Therefore, with most TAGs the electric arc attachment at the cathode is rotated by means of a magnetic field.

The anode attachment of the arc at these high pressures is actually unstable because it is not possible to create enough charge carriers in the anode layer. So one or several moving arc attachment spots are formed which would destroy the water-cooled anodes of the TAG. One can try to prevent this by "stabilizing" the anode attachment with the help of an axial magnetic field and/or a gas turbulence. This process is called stabilization, but it is actually more like a destabilization because the arc attachment is caused to move rapidly over the electrode.

In principle there are three different concepts, the hollow electrode arc heaters used for example at the DLR in Cologne [37] and at SIMOUN by Aerospatiale [38], the constricted arc plasma generators, used for example at NASA Ames [36] and the glowing rod-shaped cathode device as for example developed at the IRS and described below.

The attainable exit speed c_e of the plasma with all these TPGs is essentially dependent on two values: the mean effective molecular weight $\overline{M}_{eff}$ of the gas which corresponds to a temperature and a pressure which lies between the values in the combustion chamber and those at the nozzle end, and the attainable arc chamber temperature T_0.

In a first approximation, the exit velocity is given by:

$$c_e \cong \sqrt{\frac{2\,\kappa_{eff}}{\kappa_{eff}-1}\,\frac{R\,T_0}{\overline{M}_{eff}}} \quad , \qquad (4.1)$$

since the temperature at the nozzle exit can be considered as very low compared to the arc chamber temperature T_0. The dependence on the effective adiabatic coefficient κ_{eff} is low.

The gas used in PWK facilities is determined by the composition of the atmosphere to be simulated. The effective mean molecular weight is hereby mainly dependent on the pressure in the accelerator and the temperature by means of the dissociation and the ionization degree. It decreases as the temperature rises and the pressure falls. In order to reach high flow velocities, the temperature in the arc chamber must be as high as possible. The maximum arc chamber temperature is limited by the maximum possible cooling rate at the chamber wall.

TAGs are operated at high pressures (from several 10^5 Pa to approx. 10 MPa), high weight rates of flow (up to several kg/s) and electric power of up to a maximum of 100 MW. In order to keep the erosion of the electrodes and the electrode fall losses to an absolute minimum, the working point of a TAG is at the lowest possible current intensity because both losses are proportional to the current intensity. Therefore the necessary power for accelerating the gas is coupled in at the highest possible voltage level, usually at several kV. However, undesired discharges must be prevented which in turn limits the voltage. Thus, voltages higher than 30 kV are difficult to obtain and current intensities of several kA in larger facilities are unavoidable. This leads to a proportionately high erosion of both electrodes and consequently to a high impurity level and low electrode life times.

In order to simulate high enthalpy air flows at pressure levels above 5 kPa, which is the limit of MPGs (see section 4.2) and in heat flux ranges between 100 kW/m^2 and about 3 MW/m^2 in stagnation point configuration, a coaxial thermal plasma generator (TPG) called RB3 (Fig. 4.1) has been developed for the PWK 4. In Fig. 4.2 the nozzle part of the RB3 generator installed in PWK 4 can be seen. Figure 4.3 shows the generator in operation during a material test.

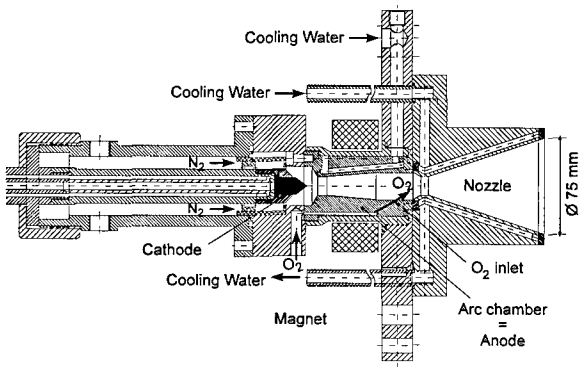

Fig. 4.1: Plasma source RB3

The test gas is heated in the discharge chamber by an electric arc and accelerated in a nozzle. In the present version a 2 % thoriated tungsten cathode is used. The anode is a water-cooled copper cylinder, whereas the nozzle is electrically insulated. Since contact between the oxygenic part of the test gas and the cathode has to be avoided, the air used for re-entry simulation is divided into two parts. As main part the nitrogen is passed along the cathode into the plenum chamber. The oxygen is injected at the downstream end of the anode towards the nozzle throat. To ensure a good mixing of the nitrogen and the oxygen, the injection point is positioned in the subsonic part of the TAG so that a backflow of oxygen into the cathode region cannot be ruled out completely. However, tests have shown that the cathode erosion rate due to the bi-throat design for RB3 is as low as observed in the MPGs operated in PWK 1 and PWK 2 and in the order of the sublimation rate [39]. To avoid anode erosion due to spotty arc attachment, a coil is used to generate an axial magnetic field which moves the arc rapidly around.

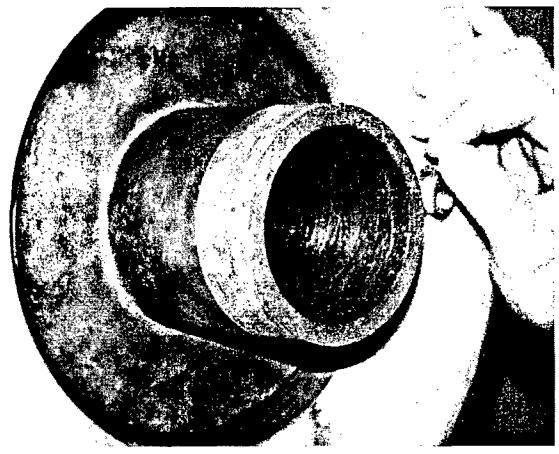

Fig. 4.2: RB3 installed in PWK 4

Fig. 4.3: RB3 in operation

The adjustable parameters in PWK 4 equipped with RB3 are the arc current, the mass flow rate, the ambient pressure and the distance to the exit of the plasma source. The arc voltage is decreasing with rising arc current and is in the order of 120 - 160 V, increasing with mass flow (Fig. 4.12). The thermal efficiency, defined as

$$\eta_{th} = \frac{P_{el} - \dot{Q}_{tot}}{P_{el}} \quad , \qquad (4.2)$$

with the total electrical input power P_{el} and the total heat losses inside the plasma source $\dot{Q}_{tot}$, is about 72 % with a mass flow rate of 5 g/s N_2/O_2 and about 82 % with 10 g/s N_2/O_2 (Fig. 4.14). It decreases slightly with increasing current due to the increase of pressure in the arc chamber, whereas the averaged specific enthalpy at the nozzle exit

$$\bar{h} = \frac{P_{el} - \dot{Q}_{tot}}{\dot{m}} \qquad (4.3)$$

increases (see Fig. 4.13). The arc chamber pressure, which determines the maximum expansion ratio, is in the order of 40 to 90 kPa, increasing with mass flow and arc current (Fig. 4.15).

The conditions in the measurement section of PWK 4, namely the stagnation pressure, the heat flux measured with a cold copper probe and the corresponding local specific enthalpy calculated with Pope's theory [40], are plotted as functions of the ambient pressure in Figs. 4.4 and 4.5 for two different mass flow rates. With 5 g/s (Fig. 4.4) at an ambient pressure of 450 Pa the maximum heat load situation of the Japanese space plane Hope can be simulated. By increasing the mass flow rate to 10 g/s (Fig. 4.5) and slightly increasing the ambient pressure, the stagnation pressure reaches ca. 10 kPa at a heat flux level of $\sim 2.2\ MW/m^2$ and a specific enthalpy of 24 MJ/kg. In order to meet the requirements of Colibri, the stagnation pressure has to be increased again by a factor of two, which can easily be done by further increasing the mass flow rate, the power and the ambient pressure.

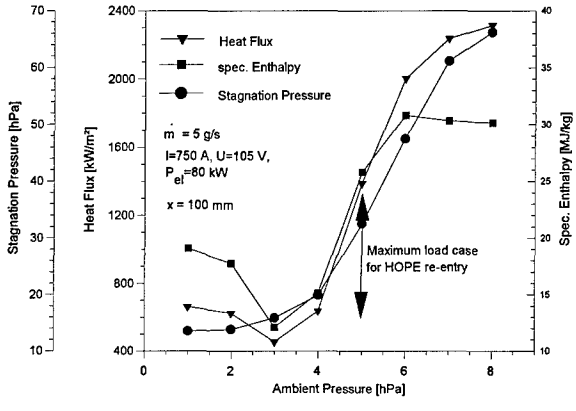

Fig. 4.4: Local specific enthalpy, heat flux and stagnation pressure as a function of the ambient pressure for a mass flow rate of 5 g/s air [2]

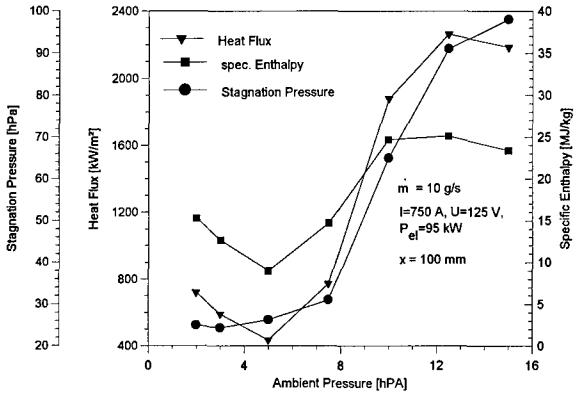

Fig. 4.5: Local specific enthalpy, heat flux and stagnation pressure as a function of the ambient pressure for a mass flow rate of 10 g/s air [2]

For the plasma generation in PWK 5 a TAG is also used. The high enthalpy flow is created by the atmospheric plasma generator APG1 [41], shown in Fig. 4.6. The design is based on an arc heater developed by Wilhelmi [42]. It consists of a water-cooled copper anode and mixing chamber and a tungsten cathode. Because of the hot cathode, only inert gases can be fed along the cathode. The ignition of the arc is performed by a Paschen breakdown as for the other TAGs and MPGs. Due to the higher chamber pressure in this device, argon is used as propellant during the ignition. The argon is then gradually replaced by the test gas. The oxygen is injected into the mixing chamber downstream behind the anode.

Two anodes with diameters of 8 mm and 10 mm are available. The current-voltage and current-power characteristic is shown in Fig. 4.7. The maximum electric power is about 46 kW. The optimal operation range with respect to the erosion of the electrodes is between 200 - 500 A. In this range averaged specific enthalpies $\bar{h}$ at the nozzle end of 6 MJ/kg up to 11 MJ/kg are generated with a total mass flow of 1.1 g/s N_2/O_2. The maximum thermal efficiency at these conditions is about 40 % [43].

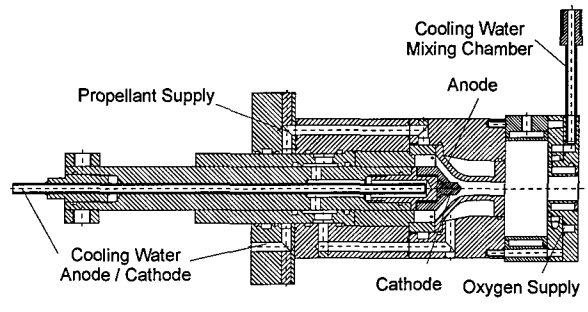

Fig. 4.6: The atmospheric plasma generator APG1 [43]

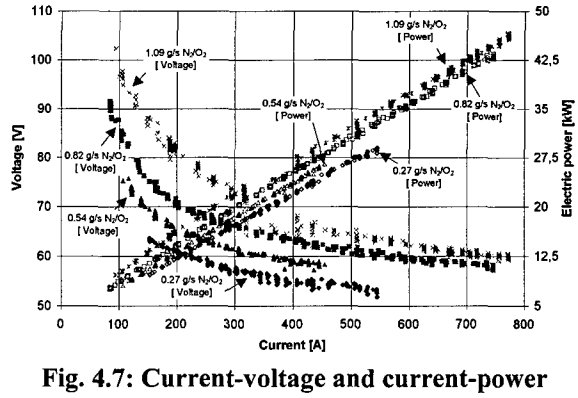

Fig. 4.7: Current-voltage and current-power characteristic, 10 mm anode, distance of the electrodes: 3 mm [43]

4.2 Magnetoplasmadynamic generators (MPG)

In the 60s and early 70s first investigations were performed to determine to what extent MPGs, being developed as plasma thrusters, were suitable for the simulation of entry conditions. Applied field as well as self-field accelerators were tested at that time [44, 45].

The acceleration principle of a self-field MPG is shown schematically in Fig. 4.8. An arc is produced between the cathode and anode of these devices. The gas is heated up, dissociated and partly ionized by the

arc within the heating chamber. The self-induced magnetic field due to the high arc current creates a Lorentz force which accelerates the plasma in the supersonic part of the nozzle in addition to the thermal acceleration through the Laval nozzle. Therefore, the attainable exit velocities are much higher compared to those with the TAG. The magnetoplasmadynamic acceleration can be shown to be proportional to the square of the current [46]. Therefore, to achieve high gas velocities, it is essential to operate at a high current level (kA).

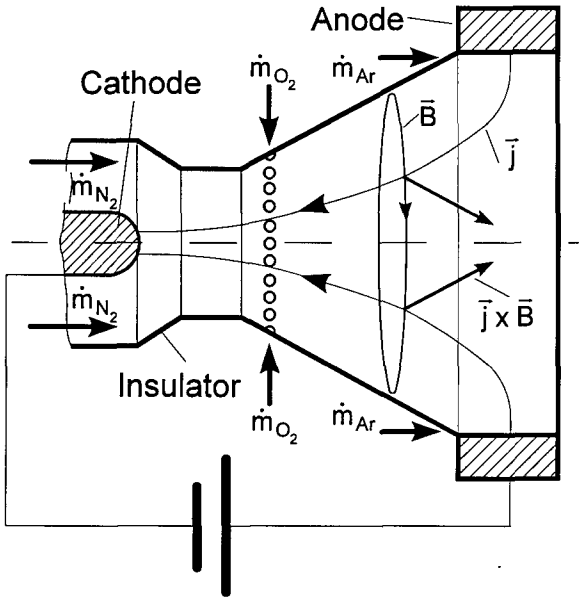

Fig. 4.8: Scheme of a self-field MPG

With the applied field MPG, an applied magnetic field is used to accelerate the plasma instead of the self-induced field in the case of a self-field MPG. Since the required densities for plasma wind tunnels are relatively high, extremely high magnetic fields of 10 - 90 T have to be generated when using an applied field MPG. At AVCO in the US, a prototype apparatus for dynamic pressures reaching nearly 1 MPa and mass flows up to 0.6 kg/s in 1 ms pulses was tested in 1970 [44]. The results were encouraging. However, the expenditure needed to run these apparatus in continuous operation mode is so great that to this day only a plasma wind tunnel in Russia has been equipped with an applied field MPG [47].

Self-field MPGs of different sizes have been developed over the past few years at the IRS. They are employed successfully in the IRS wind tunnels PWK 1 and PWK 2 for investigating erosion properties as well as ablation of heat protection materials and they are therefore looked at more closely here.

The nozzle-type MPG plasma generators (dubbed RD), as shown in Fig. 4.9, consist of two coaxial electrodes, separated by neutral, water-cooled copper segments. The nozzle exit, which is also a water-cooled segment, forms the anode. The cathode, made of 2 % thoriated tungsten, is mounted in the center of the plenum chamber.

The arc is ignited by a Paschen breakdown. The current passes through the expansion nozzle from the cathode tip to the end of the nozzle. The test gas is dissociated and partly ionized. In order to avoid the oxidation of the cathode, only the nitrogen component of the test gas is fed in along the cathode into the plenum chamber, heated up by the arc and accelerated partly by the thermal expansion and partly by the electromagnetic forces due to the self-induced magnetic field in the nozzle. The magnitude of the magnetic acceleration force strongly depends on the current level of operation [46]. With this MPG, the oxygen needed for the duplication of high enthalpy air flows is fed in radially at a high velocity at the supersonic part of the nozzle, but still within the arc region. The various gas injection points enable the operation of the MPG with different gas mixtures. As pointed out earlier this capability is used for the investigation of entry maneuvers into the atmospheres of other celestial bodies such as Titan and Mars, containing CH_4 and CO_2, respectively.

Special efforts have been made to minimize the erosion of the plasma generator. In order to avoid a spotty arc attachment on the anode, which would cause a contamination of the plasma flow, a small amount of argon is injected tangentially along the anode contour. This method has been shown experimentally to eliminate anode erosion [2]. Within the whole region of operation the only contaminating part of the MPG is the cathode. The 2 % thoriated tungsten cathode reaches more than 3000 K during the steady-state operation [39]. The high temperature and the low work function of the cathode result in a diffuse arc attachment and, consequently, a very low cathode erosion rate at the order of sublimation. Furthermore, the very low cathode erosion results in operation periods of the MPG of hundreds of hours without refurbishment of the generator.

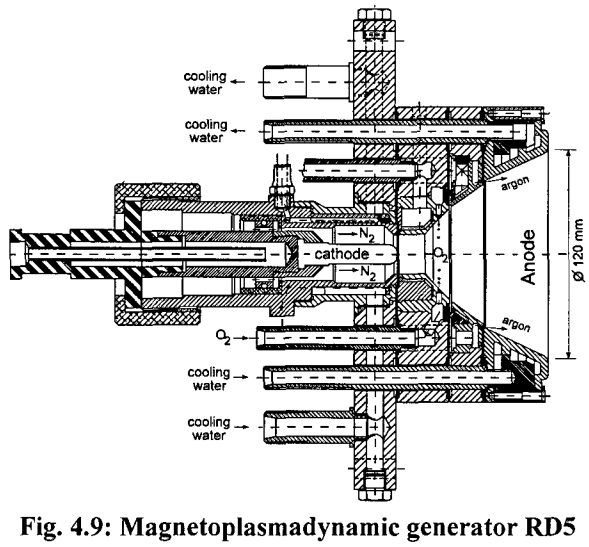

Fig. 4.9: Magnetoplasmadynamic generator RD5

The MPGs are operated at ambient pressures between 5 Pa and 5 kPa. For the MPG generator RD5, shown in Figs. 4.9 and 4.10, with a nozzle exit

diameter of 125 mm, the mass flows are between 0.3 g/s and 50 g/s at current levels between 200 A to 4000 A and power levels of 40 kW to 1 MW, while the average specific enthalpy $\bar{h}$ at the nozzle exit varies between 2 MJ/kg and 150 MJ/kg.

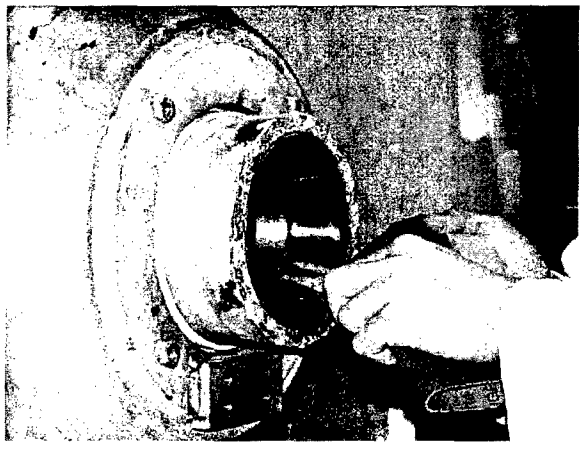

Fig. 4.10: The RD5 generator installed in the PWK

For testing large TPS structures an MPG generator with enlarged nozzle has been built. While the RD5 generator has a nozzle exit diameter of 125 mm (Fig. 4.9), the nozzle diameter of RD7 is 320 mm (Fig. 4.11), which enables the investigation of TPS materials up to 400 mm in diameter [48].

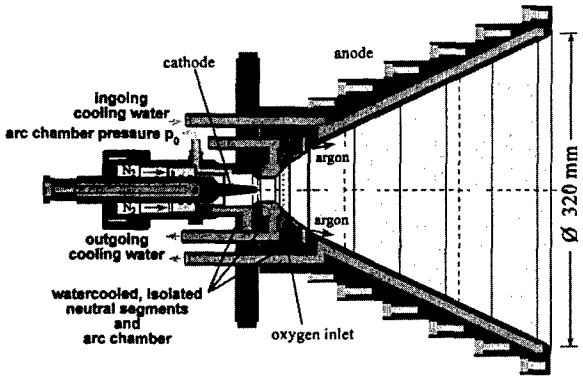

Fig. 4.11: Scheme of the plasma generator RD7

In Figs. 4.12 and 4.13 the current-voltage characteristic and the mean specific enthalpy $\bar{h}$ at the end of the plasma generator (Eq. 4.3) as a function of the current intensity are shown for various mass flows for the plasma accelerators RD5. Data of the RB3 performance are also included in these figures.

Since the degree of ionization decreases, the voltage increases with the mass flow. The specific enthalpies are dependent on the mass flow and the current intensity; low mass flow and high current intensity make it possible to reach specific enthalpies of up to 150 MJ/kg which can, for example, appear during return missions to Earth or during aerobreaking maneuvers. The specific enthalpies which are attainable with an MPG are high compared to those reached with a TAG. This can essentially be attributed to two reasons:

- additional acceleration of the gas through magnetic Lorentz forces $\vec{j} \times \vec{B}$;
- heating the gas up to the nozzle exit, which leads to a high enthalpy (and temperature) of the gas at the beginning of the free jet.

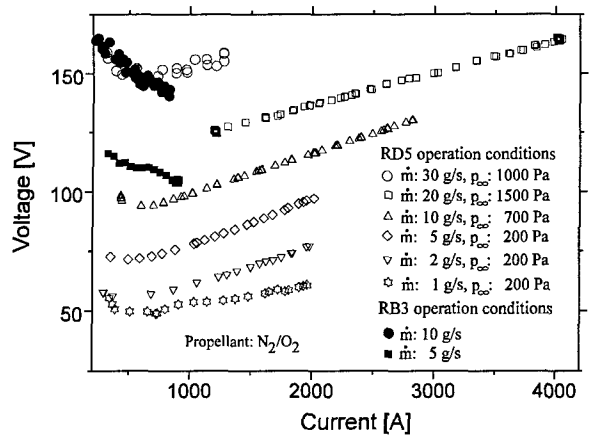

Fig. 4.12: Current-voltage characteristic of the MPG RD5 and the TPG RB3

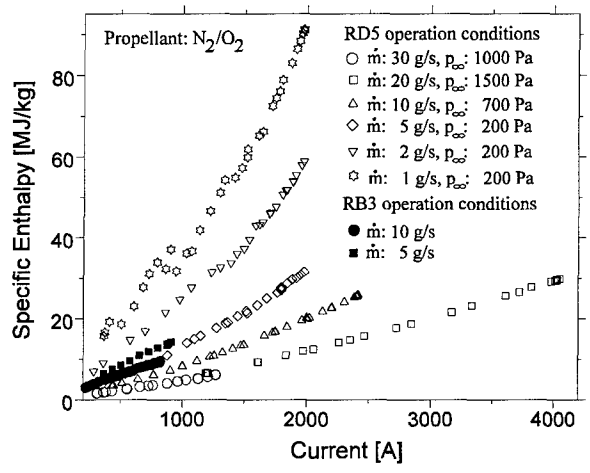

Fig. 4.13: Specific enthalpy vs. current for the MPG RD5 and the TPG RB3

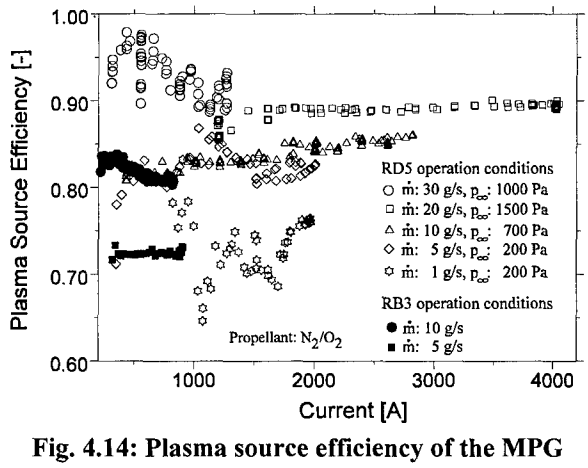

Fig. 4.14: Plasma source efficiency of the MPG RD5 and the TPG RB3

Compared to the TAG, the plasma source (or thermal) efficiency η_{th} (see Eq. 4.2) of the MPG is high. It is almost independent of the current level and lies between 70 % and 90 % (see Fig. 4.14). This is

due to the low combustion chamber pressure in the RD generator, which is dependent on the electric power and the mass flow and lies between 2 and 40 kPa (Fig. 4.15). Radiation losses do not play a role at these pressure levels.

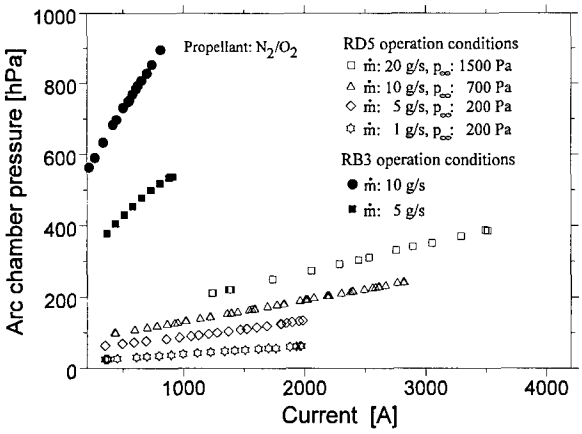

Fig. 4.15: Arc chamber pressure vs. current for RD5 and RB3

Since there are various possibilities for the gas supply for the RD-devices, these plasma sources are ideal for simulating the entry conditions into the atmospheres of other celestial bodies. In PWK 2, for example, the qualification tests were carried out for the heat shield of Huygens for the entry into the atmosphere of Saturn's moon Titan [7, 8] (Fig. 4.16). Currently, preparations are being made for a Mars mission. Both atmospheres contain carbonaceous gases.

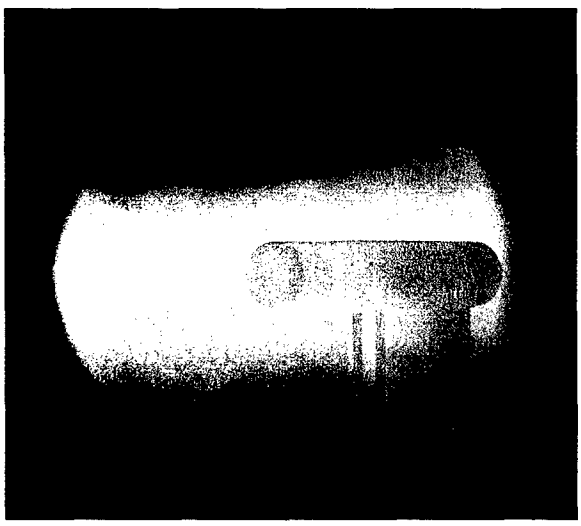

Fig. 4.16: Material test for Huygens reentry

The plasma source is also suitable for the systematic investigation of the influence of individual plasma components. Therefore, tests of kinetic effects and the influence of individual components on erosion can also be performed at the IRS. The plasma jet, created by an MPG, is neither in thermal nor in chemical equilibrium. Therefore, by investigating the plasma of different cross sections using experimental diagnostic methods, numerical non-equilibrium codes can be validated.

For further optimization of the MPGs and for the investigation of the local test conditions in MPG wind tunnels, a computational method is presently being developed [14]. This is based on numerical methods which have already been qualified for plasma thrusters [13].

4.3 The inductive plasma generator IPG

One basic aim of reentry material experiments is the investigation of the catalytic behavior. Due to the cathode erosion of the TAG and MPG generators, plasma pollution is present, which may lead to unwanted chemical reactions in front of the material probe. Therefore, an electrodeless, inductively heated plasma generator IPG, which enables the generation of metallic particle free plasma flows, has been developed at the IRS. The behavior of the probe and the plasma in front of it can be considered to be unadulterated. This means that it is possible to investigate the catalytic behavior of the TPS material and to make a comparison between the inductively heated plasma and the arc-heated plasma. The second advantage also results from the inductively coupled power input: Even rather reactive gases (oxygen, carbon dioxide) are applicable. Hence, atmospheres of celestial bodies like Mars or Venus can be simulated. The influence of the single gas components can be investigated e.g. with regard to the catalytic behavior of a material.

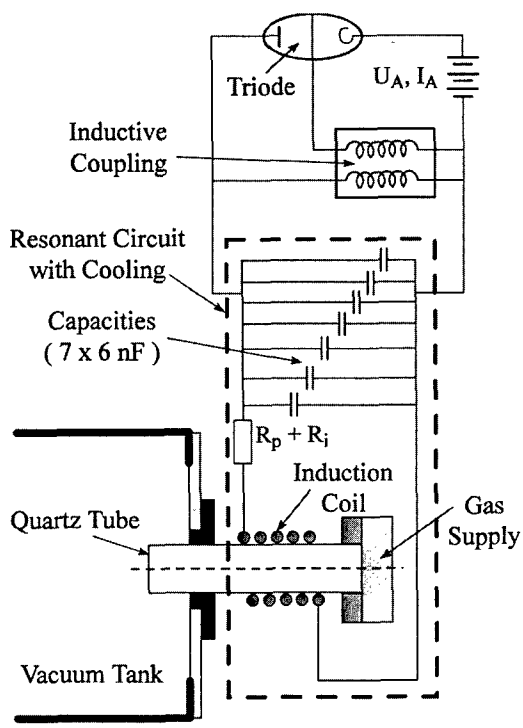

Fig. 4.17: Scheme of the induction heated plasma generation

An inductive plasma generator basically consists of an induction coil surrounding a quartz tube and

capacities, as schematically shown in Fig. 4.17. This resonant circuit is fed by an energy supply. The alternating current in the coil induces a mostly azimuthal electric field inside the quartz tube. This electric field initiates an electric discharge in the gas which is injected at one side into the tube (see Fig. 4.18). The produced plasma is expanded into the vacuum chamber. The electric discharge in the plasma is carried by mostly azimuthal currents. The current amplitude - and thus the Ohmic heating - strongly depends on the electric conductivity of the plasma and the resonant frequency of the electric circuit.

According to Lenz's law, the currents in the plasma produce a magnetic field to counteract the electromagnetic field of the induction coil. This gives rise to a limitation of the penetration depth of the external magnetic field. This so-called skin-depth δ depends on the electrical conductivity σ and the frequency f [49, 50]:

$$\delta = \sqrt{\frac{2}{\mu_0 \sigma f}} \quad . \qquad (4.4)$$

The higher the electric conductivity of the plasma and the higher the resonant frequency, the lower the skin-depth, and thus, the penetration of the external electromagnetical field into the plasma.

The plasma generator IPG3 is shown in Fig. 4.18. The gas injection head enables different gas injection angles. The quartz tube contains the produced plasma, which leaves the generator through the water-cooled vacuum chamber adapter. The induction coil is connected to the external resonant circuit, which delivers power and high pressure cooling water. Furthermore, both the tube and the coil are surrounded by the external tube cooling, which protects the tube from overheating. The total length of IPG3 is about 0.35 m, its diameter about 0.08 m.

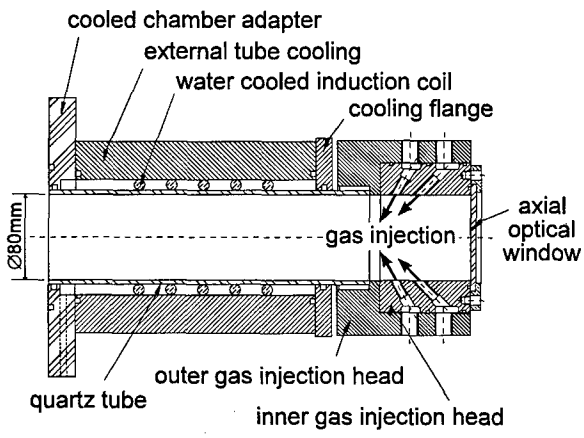

Fig. 4.18: View of the plasma source IPG3

As mentioned before, various gas injection angles are achievable by replacing the inner gas injection head with others which have different bore angles. Therefore, the influence of the injection angle on the operational behavior of IPG3 can be studied and optimized for certain applications. It is evident that the plasma is continuously swept away by an axially injected gas [49]. Using a tangential injection of the gas enables the plasma to be stabilized. Furthermore, lower pressure can be expected in the tube's center. So on the one hand the plasma recirculates, on the other hand it is kept away from the inner surface of the tube. Hence, a lower heat load of the tube can be achieved and higher power can be applied. An axial optical access through the inner injection head enables investigations of the plasma inside the generator. Figure 4.18 schematically shows the optical access and Fig. 4.19 the optical window of IPG3 while it is in operation with argon. The tube cooling system is transparent; therefore, the position of the "plasma flame" within the tube can be observed with regard to different operating parameters such as chamber pressure, gas, mass flow rate and anode power.

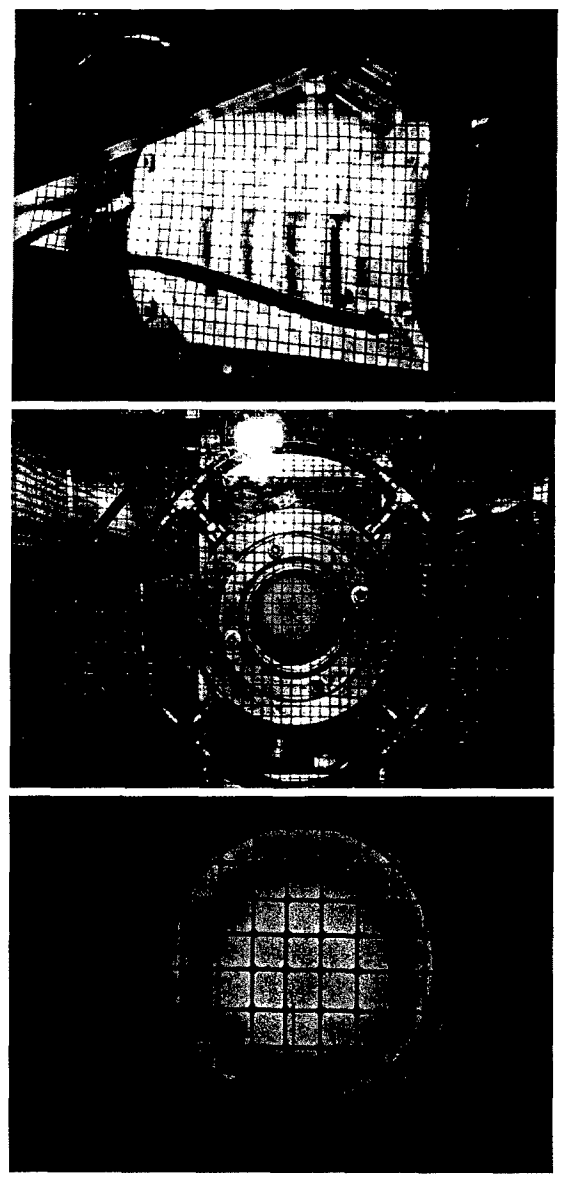

Fig. 4.19: Plasmagenerator IPG3 in operation (argon); top: side view; middle and lower: axial optical window

Additionally, this feature is supported by the axial optical window.

Figure 4.19 shows IPG3 and its tube cooling while operating with argon. The top picture in Fig. 4.19 is a side view of IPG3, the middle and lower pictures the axial optical access of IPG3.

As indicated in Fig. 4.17, the Meissner type resonant circuit is supplied by the DC anode power P_a, which is calculated from the measured anode voltage U_a and the anode current I_a during the operation of the device [24]. The anode voltage is controlled. Hence, the anode current results from the load of the resonant circuit (plasma) and the accompanying operating conditions.

The operational frequencies were measured using a Rogowski coil, which was wrapped around one of the inductor connections (see Fig. 3.4).

All measurements presented here were performed at an ambient pressure of about 100 Pa inside the vacuum chamber and with 7 capacitors switched in parallel (see Fig. 3.10). The measurements were made using air and argon with different anode powers. The gases were tangentially injected. Figure 4.20 shows the determined frequencies for argon and air versus the anode power P_a. The averaged value for the frequency in air operation is 510 kHz, the averaged value for argon is 528 kHz. The different frequencies can be most likely explained by the different field dampings due to the mutual inductions, which lead to a change of the inductivity. This again changes the operational frequency.

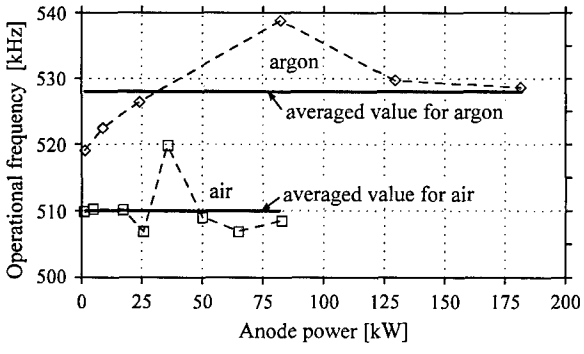

Fig. 4.20: Operational frequencies (argon and air)

A CID camera was used to investigate the discharge and to measure the radial intensity distribution of the plasma. The measurement was done through the axial optical window of IPG3. Its focus was about 0.05 m behind the closest coil winding; the camera's distance to the axial outlet was about 2.5 m. Therefore, the rf-protection cage meshes, as can be seen in Fig. 4.21, could be used as a geometric net enabling the introduction of the tube's diameter geometry. The camera has a spectral response in a wide wavelength range leading to an arbitrary intensity distribution; therefore, the data were normalized with respect to the measured maximum.

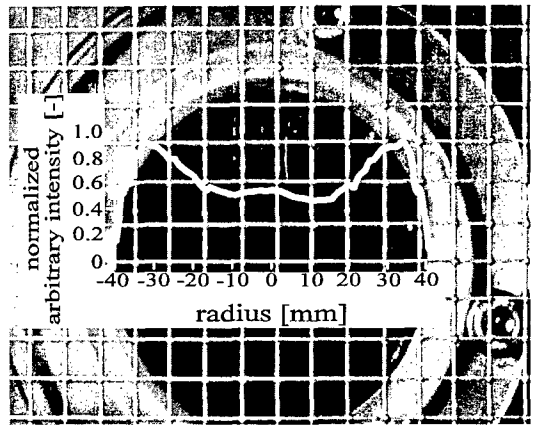

Fig. 4.21: Arbitrary intensity history along the x-direction of the optical window of IPG3 (air)

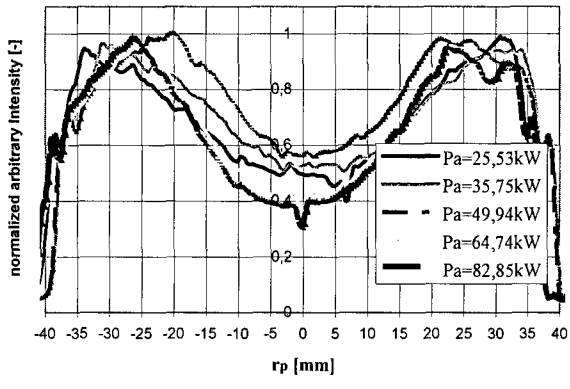

Fig. 4.22: Normalized relative intensities of the discharge for different anode powers (air)

Figure 4.22 shows the behavior of the arbitrary relative intensity curves of the discharge as a function of increasing power for air operation. Generally, the intensity of the discharge increases with the power. But the intensity "peaks" at the inner tube wall only slightly increase with increasing input power.

The anode power distribution can be written, for practical considerations, in the following form

$$P_A = f(U_A) + aU_A^2 \approx bU_A^c \quad . \qquad (4.5)$$

Here, P_A is the anode power, U_A is the measured anode voltage, the term aU_A^2 represents the real powers according to the Ohm's law, while $f(U_A)$ represents the remaining power losses such as the anode losses of the metal-ceramic triode. This leads to $P_A = bU_A^c$, with $c > 2$. This consideration is confirmed by the measured power lines (see Figs. 4.23 - 4.24), which are, in a first approximation, represented by polynomial functions depending on U_A^c. Hence, the anode powers in a double logarithmic scale appear approximately a straight lines.

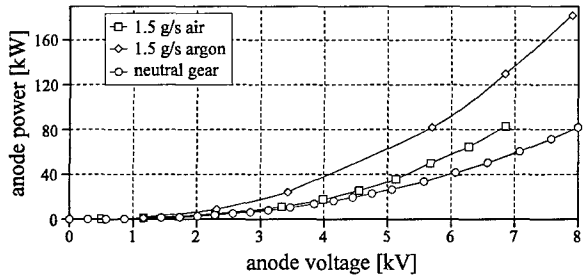

Fig. 4.23: Anode power versus anode voltage for argon, air and "plasma-off" mode

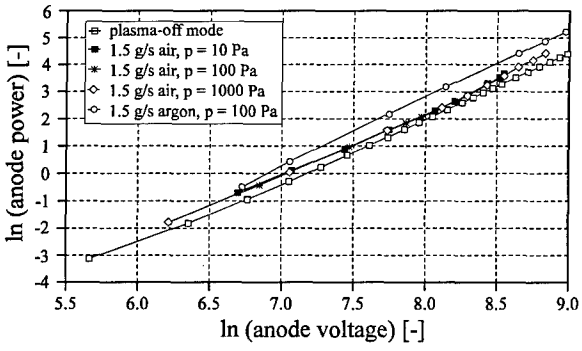

Fig. 4.24: Anode powers in logarithmic scale

4.4. Erosion of the Plasma Sources

When material tests are to be performed in a plasma wind tunnel, it is of the utmost importance that the plasma which is generated is free from impurities because they change the catalycity of the material and thus more than double the heat flux and significantly enlarge the erosion rate. Therefore, erosion on the electrodes or rather on the discharge vessel must be avoided or minimized.

Copper for example has a large catalytic effect, which means nitrogen and oxygen atoms are encouraged to form molecules on the surface releasing most of their combining energy at the surface. SiC on the other hand has a relatively small catalytic effect.

Erosion of the anode can be avoided in an MPG if the arc attachment is diffuse. In order to guarantee this with the, in some cases, relatively high pressures on the anode (to approx. 5 kPa), a small amount of argon is fed in tangentially to the anode (see Fig. 4.9). In a TAG spot formation at the anode cannot be avoided due to the high operating pressures (0.1 - 10 MPa). A destabilization of the anode attachment by means of a magnetic field and/or the turbulent movement of gas minimizes the erosion. In this way and with cooled copper anodes the erosion is minimal and a service life up to 100 hours can be achieved [46, 39].

In principle, erosion on the arc cathode is unavoidable. There are two possibilities for the arc's cathode attachment in the plasma generator: the focal spot with a cooled cathode and the diffuse attachment with primarily thermal electron emissions and a hot cathode (at cathode temperatures higher than 2000°C) [39]. In the case of the focal spot, the erosion rate of the cathode is up to three times higher than when it is operated in a hot state [39]. In both cases, the cathode erosion is almost proportional to the current intensity. Therefore, thermal arc sources are operated at a low current intensity.

Hot tungsten cathodes are in use for the small TAGs as at the IRS in order to run at the lowest possible erosion mode. The disadvantage in this case is that the gas has to be separated and only purified nitrogen may be in contact with the glowing cathode. Due to the high operation cost, this cannot be realized in large devices in the MW-level. Here undecomposed gases are used with cooled copper cathodes. The arc attachment in this case is not diffuse but rather it appears as a so-called focal spot with local melting [46]. The higher erosion, in this case copper, must be accepted.

MPGs must be operated with as high a current intensity as possible because the magnetic acceleration increases with the square of the current intensity [46]. Therefore, hot cathodes out of thoriated tungsten are always used with the MPG in order to nevertheless reach comparatively low erosion rates and good jet qualities. This is especially advantageous for material tests because tungsten oxidizes in air plasmas. Because tungsten oxide has a high vapor pressure, it doesn't settle on the hot material samples.

Figure 4.25 shows the contamination of the test gases from erosion products in various plasma wind tunnels [3]. The superiority of the PWKs equipped with MPGs is obvious. However, also the erosion rates for the RB plasma source at the IRS are rather low compared to the erosion rates of constricted and Huels-type arc generators. In addition, high productivity in the tunnel is a result of the low erosion rate because the life span of the electrodes is many hun-

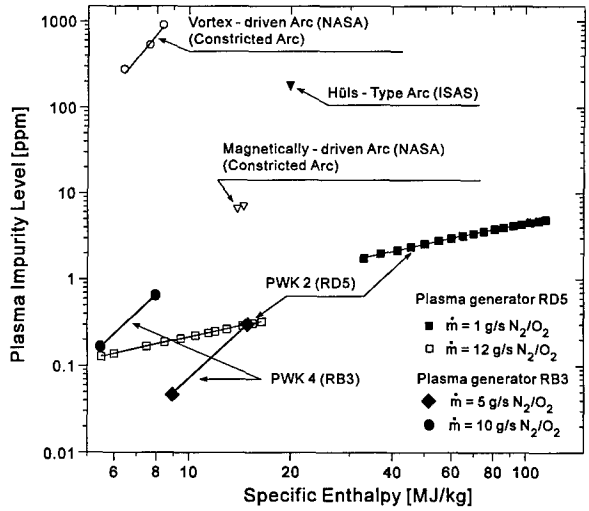

Fig. 4.25: Diagram of the plasma impurity level in the MPG driven PWK [3], data partly from [51, 52]

dreds of hours.

A disadvantage of the hot cathode is that oxygen must be kept away from it. Therefore, in the MPG purified nitrogen is fed in along the cathode while the oxygen is blown into the supersonic part of the nozzle. This part lies directly behind the narrowest cross section and consequently still within the arc. Cathode erosion tests with the MPG resulted in a significant decrease in the erosion rate down to the level of sublimation while avoiding remaining oxygen and dampness in the nitrogen [39].

In an IPG, which is operated without electrodes, indications of erosion can appear on the vessel or rather on the cooling elements which contaminate the plasma. In Russia such devices are operated with cooling inserts. Investigations of the plasma contamination are not available. At the IRS the TAG is operated without any cooling insert.

In addition to the importance of the absolute quantity of eroded material in the jet, one has to point out that different materials have different influences on the material tests. For example, copper particles ejected from arc spots are found to be partly deposited on the material probes, whereas no tungsten deposit eroded from MPG cathodes has ever been detected.

First results of a comparison of catalytic material behavior in a MPG and a TAG have shown no difference in the material behavior [3]. This indicates that the very small tungsten pollution has no influence.

Acknowledgements

The authors would like to thank all colleagues who were involved in the set-up and operation of the plasma wind tunnel facilities at the IRS. Special thanks also to Mrs. Jennifer Baer-Engel for her help in writing this script.

5. References

[1] NASA Photo Gallery, Dryden Flight Research Center, 1997

[2] M. Auweter-Kurtz, H.L. Kurtz, S. Laure, "Plasma Generators for Re-entry Simulation", Journal of Propulsion and Power, Vol. 12, No. 6, pp. 1053 - 1061, Dec. 1996

[3] S. Laure, "Experimentelle Simulation der Staupunktsströmung wiedereintretender Raumflugkörper und deren Charakterisierung mittels mechanischer Sonden", Ph.D. Dissertation, Institut für Raumfahrtsysteme, Universität Stuttgart, Germany, May 1998

[4] M. Auweter-Kurtz, H. Habiger, S. Laure, E. Messerschmid, W. Röck and N. Tubanos, "The IRS Plasma Wind Tunnels for the Investigation of Thermal Protection Materials for Reentry Vehicles", Proceedings of the 1st European Symposium on Aerothermodynamics for Space Vehicles (Noordwijk, Netherlands), European Space Agency, SP-318, Paris, France, 1991, pp. 283 - 293

[5] M. Elsner, "Thermal Protection System - Comparison of Hermes Flight Environment and Test Facility Environment of the IRS Plasma Wind Tunnel", Messerschmidt-Bölkow-Blohm, TR H-NT-1B-0006-MBB, Munich, Germany, 1990

[6] S. Laure, M. Auweter-Kurtz, H. Kurtz, "Plasma Flows for Reentry Simulation", Proceedings of the 12th International Symposium on Plasma Chemistry, Vol. 3, Univ. of Minnesota, Minneapolis, MN, 1995, pp. 1749 - 1754

[7] W. Röck, M. Auweter-Kurtz, "Experimental Investigation of the Huygens Entry into the Titan Atmosphere within a Plasma Wind Tunnel", AIAA Paper 95-2112, July 1995

[8] W. Röck, "Simulation des Eintritts einer Sonde in die Atmosphäre des Saturnmondes Titan in einem Plasmawindkanal", Ph.D. Dissertation, Institut für Raumfahrtsysteme, Universität Stuttgart, Germany, Dec. 1998

[9] M. Auweter-Kurtz, H. Hald, G. Koppenwallner, H.-D. Speckmann, "German Reentry Experiments on EXPRESS", 45th Congress of the International Astronautical Federation, 94-1.3.192, Jerusalem, Israel, Oct. 1994; published in ACTA ASTRONAUTICA, Vol. 38, No. 1, pp. 47 - 61, 1996

[10] H. Habiger, M. Auweter-Kurtz, H. Früholz, G. Herdrich, "PYREX - Pyrometric Temperature Measurement on the Ceramic TPS of the Re-Entry Capsule MIRKA", Proceedings of the 3rd European Workshop on Thermal Protection Systems, WPP-141, pp. 353 - 361, ESTEC, Noodwijk, The Netherlands, März 1998

[11] G. Herdrich, M. Auweter-Kurtz, H. Habiger, M. Hartling, "Multi-Channel Temperature Measurements on Ceramic Heat Shields", IAF-97-I.5.06, 48th International Astronautical Congress, Turin, Italy, 6-10 October 1997

[12] G. Herdrich, M. Auweter-Kurtz, M. Hartling, T. Laux, "Present Design of the Pyrometric Sensor System PYREX-KAT38 for X-38", International Symposium on Atmospheric Reentry Vehicles and Systems, Arcachon, France, March 1999

[13] C. Sleziona, "Hochenthalpieströmungen für Raumfahrtanwendungen", Habilitation, Faculty

of Aerospace Technology, University Stuttgart, 1999

[14] C. Sleziona, M. Auweter-Kurtz, E.W. Messerschmid, "Evaluation of an Air Driven Plasma Wind Tunnel Source", AIAA 96-1854, 31st AIAA Thermophysics Conference, New Orleans, June 1996

[15] T. Grau, E. Messerschmid, "Numerical Investigation of a Partially Ionized Air Flow in a Plasma Wind Tunnel", AIAA 98-2955, 7th AIAA/ASME Joint Thermophysics and Heat Transfer Conference, Albuquerque, NM, USA, June 1998

[16] S. Lenzner, M. Auweter-Kurtz, J. Heiermann, C. Sleziona, "Energy Distribution in an Inductively Heated Plasma Wind Tunnel for Re-entry Simulations", AIAA-98-2947, 7th AIAA/ ASME Joint Thermophysics and Heat Transfer Conference, Albuquerque, NM, USA, June 1998

[17] Lukasiewicz, J., Whitfield, J.D., Jackson, R., "Aerodynamic Testing at Mach Numbers from 15 to 20", Proceedings of the ARS International Hypersonic Conference, Cambridge, Massachusetts, 1961

[18] Hornung, H., "High Enthalpy Wind Tunnel for the Simulation of Chemical Nonequilibrium Effects", HEG, DLR, Institut für Experimentelle Strömungsmechanik, Document Number IB222-86A43, 1986

[19] E. Messerschmid, S. Fasoulas, "Grundlagen der Raumfahrtsysteme", Vorlesung, Institut für Raumfahrtsysteme, Universität Stuttgart, 1998

[20] M. Auweter-Kurtz, G. Hilfer, H. Habiger, K. Yamawaki, T. Yoshinaka, H.-D. Speckmann, "Investigation of Oxidation Protected C/C Heat Shields in Different Plasma Wind Tunnels", IAF-96-1.3.06, 42nd International Astronau-tical Congress, Beijing, China, October 1996, accepted for publication in ACTA ASTRONAUTICA

[21] Y. Morino, T. Yoshinaka, M. Auweter-Kurtz, G. Hilfer, H.-D. Speckmann, A. Sakai, "Erosion Characteristics of SiC Coated C/C Materials in Arc Heated High Enthalpy Air Flow", IAF-97-I.4.02, 48th International Astronautical Congress, Turin, Italy, October 1997

[22] G. Hilfer, M. Auweter-Kurtz, "Experimental and Theoretical Investigation of the Oxidation Behavior of Thermal Protection Materials under Oxygen Attack", High Temperatures - High Pressures, 1995/1996, Vol. 27/28, pp. 435 - 448, also ESA/ESTEC 2nd Workshop on Thermal Protection Systems and 3rd European Workshop on High Temperature Materials, Stuttgart, October 1995

[23] G. Herdrich, M. Auweter-Kurtz, H. Kurtz, S. Lenzner, "A Test Facility with a Newly Developed Inductively Heated Plasma Generator for TPS Re-entry Simulations", Proceedings of the 3rd European Workshop on Thermal Protection Systems, WPP-141, pp. 109 - 115, ESTEC, Noodwijk, The Netherlands, März 1998

[24] G. Herdrich, M. Auweter-Kurtz, H. Kurtz, "A New Inductively Heated Plasma Source for Re-Entry Simulations", AIAA-98-3022, 20th AIAA Advance Measurement and Ground Testing Conference, Albuquerqu, NM, June 1998

[25] M. Fertig, A. Dohr, H.-H. Frühauf, "Transport Coefficients for High Temperature Non-equilibrium Air Flows", AIAA 98-2937, 7th AIAA/ASME Joint Thermophysics and Heat Transfer Conference, Albuquerque, NM, USA, June 1998

[26] M. Auweter-Kurtz, G. Bauer, K. Behringer, P. Dabalà, H. Habiger, K. Hirsch, H. Jentschke, H. Kurtz, S. Laure, T. Stöckle, G. Volk, "Plasma-diagnostics within the Plasma Wind Tunnel PWK", Zeitschrift für Flugwissenschaften und Weltraumforschung, Vol. 19, No. 3, pp. 166 - 179, June 1995

[27] M. Auweter-Kurtz, H. A. Habiger, Th. Wegmann, "Diagnostics of High Enthalpy Plasma Flows", AIAA 97-2495, 32nd Thermo-physics Conference, Atlanta, GA, USA, June 1997

[28] H. Hald, P. Winkelmann, "Post Mission Analysis of the Heat Shield Experiment CETEX for the EXPRESS Capsule", IAF-97-I.4.01, 48th International Astronautical Con-gress, Turin, Italy, October 1997

[29] J. Burkhardt, U. Schöttle, E. Messerschmid, "Mission and System Design Aspects of a Semi-Ballistic Reentry Experiment Vehicle", 48th International Astronautical Congress, Turin, Italy, October 1997

[30] M. Auweter-Kurtz, "Cassini-Huygens-Mission - Qualifikation des Hitzeschutzes für den Eintritt in die Atmosphäre des Titan", Revue Technique, Vol. 3, pp. 145 - 153, Luxemburg, March 1993

[31] M. Auweter-Kurtz, S. Laure, W. Röck, "Experimental Planet Entry Simulation within a Plasma Wind Tunnel", ESA SP-367, Proc. of the 2nd European Symposium on Aerothermo-dynamics for Space Vehicles, ESTEC, Noordwijk, The Netherlands, November 1994

[32] G. Francois, J.P. Ledy, A. Masson, "ONERA High Enthalpy Wind Tunnel F4", 82th Meeting of the Supersonic Tunnel Association, October 1994

[33] Finklenburg, W., Peter, T., "Kontinuierliche Spektren", Handbuch der Physik, Bd. XXVII, S. 100, Springer, Berlin, 1957

[34] F. Vilbig "Lehrbuch der Hochfrequenztechnik", Vol. 2, Akademische Verlagsges.m.b.H., Frankfurt am Main, 1958

[35] "Technical Specification of the rf-capacitors and the Triode RS 3300 CJ of the PWK3-IPG energy supply", Fritz Düsseldorf Ges. m. b. H., 1997

[36] W. Winovich, W.C.A. Carlson, "The 60 MW Shuttle Inetraction Heating Facility", Proceedings of the 25th International Instrumentation Symposium (Anaheim, CA), ISBN 97664-434-5, 1979

[37] M. Fiebig, K. Kindler, D.G. Papanikas, "Hochleistungsbrenner und Expansionsdüsen zur Untersuchung von Hochenthalpieströmungen", DLR-Mitteilung 75-06, 1975

[38] "Plasma Arc Heater", Firmenbroschüre, Aerospatiale, Les Mureaux, Frankreich, 1987

[39] M. Auweter-Kurtz, B. Glocker, H. L. Kurtz, O. Loesener, H. O. Schrade, N. Tubanos, Th. Wegmann, D. Willer, J. E. Polk, "Cathode Phenomena in Plasma Thrusters", Journal of Propulsion and Power, Vol. 9, No. 6, pp. 882 - 888, 1993

[40] R.B. Pope, "Measurement of Enthalpy in Low_density Arc-Heated Flows", AIAA Journal, Vol. 6, No. 1, pp. 103 - 109, 1968

[41] M. Auweter-Kurtz, H. Wilhelmi, D. Wagels, T. Laux, "Untersuchung der Stabilität von pulvermetallurgisch hergestellten, gradierten Thermalschutzkacheln, bei thermomecha-nischer Belastung von hochenergetischen Strömungen im Hochenthalpie-Windkanal", IRS-97-Ib-19, 1997

[42] H. Wilhelmi, D. Wagels, "Untersuchung der Stabilität von pulvermetallurgisch hergestellten, gradierten Thermalschutzkacheln, bei thermomechanischer Belastung von hochenergetischen Strömungen im Hochenthalpie-Windkanal", Zwischenbericht Wi 491/34-1, Institut für Industrieofenbau und Wärmetechnik, RWTH Aachen, 1996

[43] M. Auweter-Kurtz, F. Hammer, G. Herdrich, H. Kurtz, T. Laux, E. Schreiber, Th. Wegmann, "The Ground Test Facilities for TPS at the Institut für Raumfahrtsysteme", 3rd European Symposium on Aerothermodynamics for Space Vehicles, ESTEC, Noordwijk, NL, November 1998

[44] E. R. Pugh, R. M. Patrick, A. M. Schneiderman, "High-Pressure, High-Enthalpy Test Facility", AIAA Journal, Vol. 9, No. 2, 1971

[45] H. Hügel, "Arc-Heater for High-Enthalpy Plasma Flows", Third International Conference on Gas Discharges, London, 1974

[46] M. Auweter-Kurtz, "Lichtbogenantriebe für Weltraumaufgaben", B.G. Teubner Verlag, ISBN 3-519-06139-2, 1992

[47] N. Anifimov, "TSNIIMASH Capabilities for Aerogasdynamical and Thermal Testing of Hypersonic Vehicles", AIAA 92-3962, 17th Ground Testing Conf., Nashville, July 1992

[48] M. Auweter-Kurtz, H. Habiger, G. Herdrich, G. Hilfer, H. Kurtz, S. Laure, E. Schreiber, Th. Wegmann, "The Magnetoplasmadynamic Generator RD7 - A new plasma source for large structure testing", Proceedings of the 3rd European Workshop on Thermal Protection Systems, WPP-141, pp. 101 - 108, ESTEC, Noodwijk, The Netherlands, März 1998

[49] J. Mostaghimi, M. I. Boulos, "Two-Dimensional Electreomagnetic Field Effects in Induction Plasma Modelling", Plasma Chemistry and Plasma Processing, Vol. 9, No. 1, pp. 25 - 44, 1989

[50] M. P. Freeman, J. D. Chase, "Energy-Transfer Mechanism and Typical Operating Characteristics for the Thermal rf Plasma Generator", Journal of Applied Physics, Vol. 39, No. 1, p. 180, Jan. 1968

[51] M. Hinada, Y. Inatani, T. Yamada, K. Hiraki, "Performance Characteristics of the ISAS Huels-type Arc Heater", ISTS 94-d-37, 19th International Symposium on Space Technologie and Science, Yokohama, Japan, May 1994

[52] T.J. Stahl, W. Winovich, G. Russo, S. Caristia, "Design and Performance Characteristics of the CIRA Plasma Wind Tunnel", AIAA-91-2272, AIAA/SAE/ASME/ASEE 27th Joint Propulsion Conference, Sacramento, CA, 1991